

# Technical Reference on Hydrogen Compatibility of Materials

Austenitic Stainless Steels:  
21-6-9 (code 2202)

Prepared by:  
C. San Marchi, Sandia National Laboratories

Editors  
C. San Marchi  
B.P. Somerday  
Sandia National Laboratories

This report may be updated and revised periodically in response to the needs of the technical community; up-to-date versions can be requested from the editors at the address given below. The success of this reference depends upon feedback from the technical community; please forward your comments, suggestions, criticisms and relevant public-domain data to:

Sandia National Laboratories  
Matls Tech Ref  
C. San Marchi (MS-9402)  
7011 East Ave  
Livermore CA 94550.

This document was prepared with financial support from the Safety, Codes and Standards program element of the Hydrogen, Fuel Cells and Infrastructure program, Office of Energy Efficiency and Renewable Energy; Pat Davis is the manager of this program element. Sandia is a multiprogram laboratory operated by Sandia Corporation, a Lockheed Martin Company, for the United States Department of Energy under contract DE-AC04-94AL85000.

## IMPORTANT NOTICE

**WARNING:** Before using the information in this report, you must evaluate it and determine if it is suitable for your intended application. You assume all risks and liability associated with such use. Sandia National Laboratories make **NO WARRANTIES** including, but not limited to, any Implied Warranty or Warranty of Fitness for a Particular Purpose. Sandia National Laboratories will not be liable for any loss or damage arising from use of this information, whether direct, indirect, special, incidental or consequential.

## 1. General

21Cr-6Ni-9Mn (21-6-9) is a stable austenitic stainless steel that is alloyed with nitrogen to provide superior strength compared to the standard 300-series stainless steels. The Cr+Ni content of 21-6-9 results in a relatively low stacking fault energy compared to more highly alloyed austenitic stainless steels such as type 316 stainless steel and 22Cr-13Ni-5Mn (22-13-5) [1-3]. Austenitic stainless steels with low stacking fault energy are more susceptible to hydrogen embrittlement, a feature generally attributed to non-uniform plastic deformation [1, 4]. Thermomechanical processing of 21-6-9 stainless steel results in shorter dislocation slip distances (due to increased dislocation density) and has been reported to improve ductility of material with internal hydrogen [4]. Other studies, however, show no clear benefit of worked microstructures with respect to hydrogen embrittlement and the general trend is that resistance to hydrogen embrittlement is less for higher yield strength [5-8].

The nitrogen content of 21-6-9 stainless steel is an important variable for hydrogen compatibility as high nitrogen contents are reported to significantly lower the resistance to hydrogen embrittlement [1]. Tensile testing shows that heats of 21-6-9 with nitrogen content  $>0.3\text{wt}\%$  have substantially lower ductility in the presence of hydrogen than heats with  $<0.3\text{wt}\%$  nitrogen [1]. This trend may be related to the effect of nitrogen on the stacking fault energy and associated plastic deformation behavior [1, 9].

The effect of hydrogen on 21-6-9 stainless steel appears to be very sensitive to microstructural and compositional variables; consequently, compositional variations from heat-to-heat result in the wide range of reported hydrogen-effects on tensile properties [6]. The general trends outlined above indicate that high nitrogen content ( $>0.3\text{wt}\%$ ) reduces resistance to hydrogen embrittlement. Other data suggest that nickel is generally important for resistance to hydrogen embrittlement in austenitic stainless steels [7, 10, 11]. Considering that nickel and chromium increase stacking fault energy [2, 3], high nickel and chromium content in 21-6-9 stainless steel is expected to be beneficial for resistance to hydrogen embrittlement. Finally, 21-6-9 in low strength conditions will generally have greater resistance to hydrogen effects.

### 1.1 Composition

Table 1.1.1 lists specified compositional ranges for 21-6-9 stainless steel as well as compositions of several heats of 21-6-9 used to study hydrogen effects.

### 1.2 Other designations

Nitronic 40, UNS S21900 (ASTM XM-10)  
21-6-9LC, UNS S21904 (ASTM XM-11)  
Nitronic 40W, UNS 21980 (filler wire ER219)  
Similar alloy: 21-7-9

## 2. Permeability and Solubility

The permeability of stainless steel is briefly reviewed in Refs. [11-13]; diffusivity and solubility are briefly reviewed in Refs. [11, 13]. Permeability, diffusivity and solubility can be described by standard Arrhenius-type relationships. Solubility data are normally determined from the ratio of permeability and diffusivity.

Permeability appears to be nearly independent of the composition and microstructure for stable austenitic stainless steels [13, 14]. Nitrogen additions to type 304 [14] and type 316 [13] stainless steels do not significantly affect the permeability and solubility of these alloys. The nitrogen-strengthened stainless steels 21-6-9 and 22-13-5, on the other hand, have a significantly higher measured hydrogen concentration compared to 304L when exposed to identical high pressure and temperature [15]. This higher hydrogen concentration should translate into higher solubility. Ref. [11] proposes a solubility relationship based on hydrogen concentration measurements from hot extraction of 21-6-9 with internal hydrogen (thermally precharged from hydrogen gas), Table 2.1. Hydrogen concentrations measured by hot extraction methods are summarized in Table 2.2.

Relationships for permeability (Figure 2.1) and solubility (Figure 2.2) fit to data for several austenitic stainless steel alloys from several studies are given in Table 2.1. It is important to note that these data are determined at elevated temperature and low pressure; they are extrapolated for use near room temperature and high pressure. For this reason, it is recommended that the relationships from Refs. [14, 16], Table 2.1, be used for extrapolation to low temperature since these provide conservative estimates (high values) of permeability and solubility when extrapolated. At elevated temperature, the solubility relationships from Refs. [11, 16] are recommended.

### 3. Mechanical Properties: Effects of Gaseous Hydrogen

#### 3.1 Tensile properties

##### 3.1.1 Smooth tensile properties

In general, smooth tensile properties of 21-6-9 stainless steel are only modestly affected by external hydrogen gas. High-pressure external hydrogen gas slightly increases (or has negligible effect upon) the yield and ultimate strength of 21-6-9 stainless steel, Table 3.1.1.1. Ductility, on the other hand, is slightly reduced when measured in external hydrogen gas. These trends are amplified for 21-6-9 stainless steel with internal hydrogen (tested in air or external hydrogen gas after thermal precharging in hydrogen gas): yield strength may be significantly increased with somewhat lower increases in ultimate strength, while ductility can be substantially reduced compared to material not exposed to hydrogen, Table 3.1.1.2. These effects can be attributed to the high concentration of internal hydrogen that is obtained by thermal precharging, since hydrogen concentration increases exponentially with temperature. The effect of high internal hydrogen concentrations from thermal precharging is clearly demonstrated for smooth tensile properties in Figure 3.1.1.1: the strength increases and the ductility decreases as the external pressure of hydrogen gas is increased and these effects are further magnified with internal hydrogen.

The effect of hydrogen on tensile ductility strongly depends on the microstructural condition and composition of 21-6-9 stainless steel. Annealed microstructures tend to be less susceptible to hydrogen embrittlement than worked microstructures [5, 8]: the RRA of 21-6-9 stainless steel with internal hydrogen is generally greater for annealed than for worked microstructures as shown in Figure 3.1.1.2. Warm-working by high energy rate forging (HERF) has been reported

to improve both strength and resistance to hydrogen embrittlement [4]; however, a full characterization of the materials tested in those studies was not provided and the results should be viewed as the exception rather than the rule. The data in Figure 3.1.1.2 rather show a general trend of greater susceptibility to hydrogen embrittlement as the yield strength is increased as by warm-working. There is significant uncertainty in these basic trends, however, as exemplified by the data shown in Table 3.1.1.3 for a single heat of 21-6-9 stainless steel processed to several different microstructural conditions [6]; also plotted in Figure 3.1.1.2. For this data the ductility loss of 21-6-9 with internal hydrogen and tested in external hydrogen gas indeed decreases as yield strength increases, however, cold-worked plate has the highest yield strength and is almost unaffected by hydrogen. Similarly, as show in Figure 3.1.1.2, materials with yield strength over 800 MPa have RRA that range from about 0.20 to 0.95. The broad range of response for material exposed to hydrogen can be partly explained by compositional variations.

West and Louthan performed tensile testing on a large number of heats of 21-6-9 stainless steels (data in Tables 3.1.1.1, 3.1.1.3 and 4.2.1) and found that susceptibility to hydrogen embrittlement could vary significantly depending on test variables and microstructure [6]. Although the nominal compositions of all the heats of 21-6-9 stainless steel that were tested in that study were similar, one heat differed from the others in having less nickel. This low-nickel heat of 21-6-9 also suffered the greatest loss in ductility when exposed to internal hydrogen; the lowest three points in Figure 3.1.1.2 represent this relatively low-nickel grade, heat W82a [6]. Higher nickel and chromium are known to strongly increase the stacking fault energy of stainless steels [2, 3] enhancing uniform deformation, a feature that is generally associated with greater resistance to hydrogen embrittlement [1, 4, 7].

High nitrogen content in 21-6-9 stainless steel significantly increases susceptibility to hydrogen embrittlement in smooth tensile specimens. Smooth tensile properties are plotted in Figure 3.1.1.3 for several heats of annealed 21-6-9 stainless steel that differ primarily in nitrogen content; data is also given in Table 3.1.1.4. Heats of 21-6-9 stainless steel with nitrogen levels  $>0.35\text{ wt}\%$  suffer ductility (RA) losses greater than 50%, while heats with nitrogen  $<0.35\text{ wt}\%$  experience a reduction in ductility of about 20% [1]. In addition, deformation mode and fracture mode were found to correlate with nitrogen content: heats with low nitrogen ( $<0.25\text{ wt}\%$  N) exhibited uniform deformation and exhibit ductile fracture processes in the presence of both internal and external hydrogen, while heats with high nitrogen ( $>0.35\text{ wt}\%$  N) exhibited non-uniform deformation and, when exposed to hydrogen, intergranular fracture [1]. While nitrogen appears to have an important effect on hydrogen embrittlement it should not be considered without regard to other alloying elements, such as nickel and chromium.

The magnitude of temperature effects on hydrogen embrittlement in tensile testing certainly depends on compositional and microstructural variables. The scatter in the temperature effects shown in Figure 3.1.1.4 and Table 3.1.1.5 might be explained by differences in composition or microstructure if that information were known. The trend for ductility loss measured from smooth tensile specimens of 21-6-9 stainless steels appears to be a minimum at a temperature between 200 K and 250 K, Figure 3.1.1.4. The ductility of 21-6-9 stainless steel with internal hydrogen at low (77 K) and elevated (380 K) temperature is similar to that at room temperature. The effect of temperature on smooth tensile properties of a heat of 21-6-9 stainless steel that is relatively unaffected by internal hydrogen is shown in Figure 3.1.1.5.

Strain rate does not have a large impact on the loss of ductility of 21-6-9 stainless steel with internal hydrogen at conventional rates, e.g.,  $<0.001 \text{ s}^{-1}$ , Figure 3.1.1.6. At higher strain rates the ductility is substantially improved; this is interpreted as a consequence of high velocity dislocations separating from hydrogen atmospheres [17].

### 3.1.2. Notched tensile properties

Notched tensile specimens with internal hydrogen (thermal precharging in hydrogen gas) show small decreases in ductility and no loss in strength, Figure 3.1.2.1. The modest hydrogen embrittlement for this particular alloy is expected since the nitrogen content is relatively low (about 0.25 wt%) and the strength is also low (yield strength of about 400 MPa). The basic trends outlined above for smooth tensile properties (susceptibility to hydrogen embrittlement increasing with nitrogen content and yield strength, but decreasing with nickel and chromium content) are expected in more comprehensive testing of notched specimens.

## 3.2 Fracture mechanics

### 3.2.1 Fracture toughness

Fracture toughness of 21-6-9, measured in high-pressure (external) hydrogen gas, exhibits a modest decrease of about 20% compared to tests in air, Table 3.2.1.1. Details of these tests were not provided other than the C-specimen geometry.

J-integral fracture toughness of high-energy-rate forgings (HERF) has been reported to strongly depend on the orientation of the microstructure and to be significantly reduced when measured in external hydrogen gas with internal hydrogen (or deuterium, thermally precharged in gas) [7, 18]. Due to the difficulty of instrumenting fracture mechanics specimens in high-pressure hydrogen gas, the  $J_m$  and tearing modulus ( $dJ/da$ ) at maximum load are used in that study for comparison of orientations and testing conditions (values at maximum load do not represent a standardized fracture toughness). Nonetheless, it was observed that in most cases testing in external hydrogen gas with internal hydrogen produced a greater effect on both the fracture toughness and the tearing modulus than testing in hydrogen gas without internal hydrogen.

### 3.2.2 Threshold stress intensity factor

Low-strength austenitic alloys ( $<700 \text{ MPa}$ ) have high resistance to crack extension in external hydrogen gas under static loads [19]. Data for 21-6-9 stainless steel are given in Table 3.2.2.1. For the one material tested, however, the forging temperature was in the range of rapid  $\beta$ -phase transformation (see section 4.2), which may explain the low ductility reported for this material.

## 3.3 Fatigue

No known data in hydrogen gas.

## 3.4 Creep

No known data in hydrogen gas.

### 3.5 Impact

Impact fracture data show a modest effect of internal hydrogen for 21-6-9, Table 3.5.1. The fracture energy at liquid nitrogen temperature is not strongly affected by the presence of internal hydrogen and is about one-third of the fracture energy at room temperature. Compositional and microstructural details of the materials tested are not reported.

### 3.6 Disk rupture tests

Disk rupture tests of 21-6-9 stainless steel display slight to moderate reductions in rupture pressure when pressurized with hydrogen compared to helium, even in heats with high nitrogen content, heat A87 [20].

## 4. Metallurgical Considerations

### 4.1 Primary processing

Microstructural features such as flow lines can have a significant effect on fracture toughness in air and on material with internal hydrogen; therefore, microstructural orientation is an important design consideration. As discussed in the section 3.1.1, 21-6-9 stainless steel in low-strength conditions generally appears to be less susceptible to hydrogen embrittlement.

### 4.2 Heat treatment

Processing temperatures for 21-6-9 stainless steel need to be controlled, particularly heating through the temperature range 773K to 1173K. Stainless steels are said to be sensitized when extensive carbide precipitation occurs in the microstructure [21]. Carbides form particularly on grain boundaries at elevated temperature (roughly 773K to 1073K), as a result, for example, of improper heat treatment, of heating slowly through this temperature range during annealing, and of welding processes. Sensitization compromises fracture properties of stainless steel as well as significantly reducing corrosion resistance. Figure 4.2.1 shows that sensitization reduces the ductility of 21-6-9 stainless steel; the ductility of sensitized microstructures is further reduced only slightly by the combination of internal and external hydrogen. Data from Figure 4.2.1 are also given in Table 4.2.1.

In addition to carbide formation, ferrite in 21-6-9 stainless steel may rapidly transform to brittle  $\delta$ -phase in the temperature range of about 923K to 1173K [22]. This transformation occurs rapidly in deformed microstructures thus heat input during welding should be carefully controlled. The  $\delta$ -phase degrades the ductility of the material independently of hydrogen exposure.

### 4.3 Properties of welds

Refs. [23, 24] report properties of gas tungsten arc (GTA) welds of 21-6-9 stainless steel with 308L and 21-6-9 filler wires measured in external hydrogen gas with and without internal hydrogen; smooth tensile properties are provided in Table 4.3.1. The loss in ductility in these tensile tests correlates well with expected hydrogen content, i.e., the ductility decreases as hydrogen content increases due to higher hydrogen pressure. Fracture of the welds in the absence of hydrogen was by microvoid coalescence (ductile fracture processes). Detailed fractography

shows failure to be associated with ferrite-austenite interfaces; fracture, however, remained primarily ductile[23, 24].

In a separate study [25], smooth and notched tensile testing of GTA and EB (electron beam) welds in 21-6-9 stainless steel revealed significantly lower ductility and slightly lower strength of the weld material compared to the base material (heat V72). Tests in high-pressure (external) hydrogen gas (69MPa), however, revealed no effect on the smooth and notched tensile strength and ductility. Static loading of both notched and smooth tensile specimens in 69MPa hydrogen gas to the yield point for 300 hours and subsequent testing in air also showed no change in properties of the base metal and the welds. Plane *stress* fracture toughness similarly showed no evidence of hydrogen effects. In all cases fracture surfaces revealed only ductile fracture processes and no evidence of secondary cracking or changes in fracture morphology due to testing in hydrogen. This study shows remarkably little effect of hydrogen compared to other studies.

## 5. References

1. BC Odegard, JA Brooks and AJ West. The Effect of Hydrogen on Mechanical Behavior of Nitrogen-Strengthened Stainless Steel. in: AW Thompson and IM Bernstein, editors. Proceedings of an International Conference on Effect of Hydrogen on Behavior of Materials, 1975, Moran WY. The Metallurgical Society of AIME (1976) p. 116-125.
2. RE Schramm and RP Reed. Stacking Fault Energies of Seven Commercial Austenitic Stainless Steels. Metall Trans 6A (1975) 1345-1351.
3. CG Rhodes and AW Thompson. The Composition Dependence of Stacking Fault Energy in Austenitic Stainless Steels. Metall Trans 8A (1977) 1901-1905.
4. MR Louthan, GR Caskey, JA Donovan and DE Rawl. Hydrogen Embrittlement of Metals. Mater Sci Eng 10 (1972) 357-368.
5. AJ West and MR Louthan. Dislocation Transport and Hydrogen Embrittlement. Metall Trans 10A (1979) 1675-1682.
6. AJ West and MR Louthan. Hydrogen Effects on the Tensile Properties of 21-6-9 Stainless Steel. Metall Trans 13A (1982) 2049-2058.
7. GR Caskey. Hydrogen Compatibility Handbook for Stainless Steels (DP-1643). EI du Pont Nemours, Savannah River Laboratory, Aiken SC (June 1983).
8. MJ Morgan. The Effects of Hydrogen Isotopes and Helium on the Flow and Fracture Properties of 21-6-9 Stainless Steel. in: PK Liaw, JR Weertman, HL Marcus and JS Santner, editors. Proceedings of the Morris E. Fine Symposium. Warrendale PA: TMS (1991).
9. RE Stoltz and JB VanderSande. The Effect of Nitrogen on Stacking Fault Energy of Fe-Ni-Cr-Mn Steels. Metall Trans 11A (1980) 1033-1037.
10. GR Caskey. Hydrogen Damage in Stainless Steel. in: MR Louthan, RP McNitt and RD Sisson, editors. Environmental Degradation of Engineering Materials in Hydrogen. Blacksburg VA: Laboratory for the Study of Environmental Degradation of Engineering Materials, Virginia Polytechnic Institute (1981) p. 283-302.
11. GR Caskey. Hydrogen Effects in Stainless Steels. in: RA Oriani, JP Hirth and M Smailowski, editors. Hydrogen Degradation of Ferrous Alloys. Park Ridge NJ: Noyes Publications (1985) p. 822-862.

12. AD LeClaire. Permeation of Gases Through Solids: 2. An assessment of measurements of the steady-state permeability of H and its isotopes through Fe, Fe-based alloys, and some commercial steels. *Diffusion and Defect Data* 34 (1983) 1-35.
13. XK Sun, J Xu and YY Li. Hydrogen Permeation Behaviour in Austenitic Stainless Steels. *Mater Sci Eng A114* (1989) 179-187.
14. MR Louthan and RG Derrick. Hydrogen Transport in Austenitic Stainless Steel. *Corros Sci* 15 (1975) 565-577.
15. GR Caskey and RD Sisson. Hydrogen Solubility in Austenitic Stainless Steels. *Scr Metall* 15 (1981) 1187-1190.
16. T-P Perng and CJ Altstetter. Effects of Deformation on Hydrogen Permeation in Austenitic Stainless Steels. *Acta metall* 34 (1986) 1771-1781.
17. JH Holbrook and AJ West. The Effect of Temperature and Strain Rate on the Tensile Properties of Hydrogen Charged 304L, 21-6-9, and JBK 75. in: IM Bernstein and AW Thompson, editors. *Proceedings of the International Conference on Effect of Hydrogen on Behavior of Materials: Hydrogen Effects in Metals, 1980*, Moran WY. The Metallurgical Society of AIME (1980) p. 655-663.
18. MR Dietrich, GR Caskey and JA Donovan. J-Controlled Crack Growth as an Indicator of Hydrogen-Stainless Steel Compatibility. in: IM Bernstein and AW Thompson, editors. *Proceedings of the International Conference on Effect of Hydrogen on Behavior of Materials: Hydrogen Effects in Metals, 1980*, Moran WY. The Metallurgical Society of AIME (1980) p. 637-643.
19. MW Perra. Sustained-Load Cracking of Austenitic Steels in Gaseous Hydrogen. in: MR Louthan, RP McNitt and RD Sisson, editors. *Environmental Degradation of Engineering Materials in Hydrogen*. Blacksburg VA: Laboratory for the Study of Environmental Degradation of Engineering Materials, Virginia Polytechnic Institute (1981) p. 321-333.
20. PF Azou and JP Fidelle. Very low strain rate hydrogen gas embrittlement (HGE) and fractography of high-strength, mainly austenitic stainless steels. in: MR Louthan, RP McNitt and RD Sisson, editors. *Environmental Degradation of Engineering Materials III, 1987*, The Pennsylvania State University, University Park PA. The Pennsylvania State University, University Park PA p. 189-198.
21. RA Lula. *Stainless Steel* (revised from "An Introduction to Stainless Steel" by JG Parr and A Hanson). Metals Park OH: American Society for Metals (1986).
22. CL Ferrera. The Formation and Effects of Sigma Phase in 21-6-9 Stainless Steel (PMT-87-0017). Rockwell International, Rocky Flats Plant, Golden CO (November 1987).
23. JA Brooks and AJ West. Hydrogen Induced Ductility Losses in Austenitic Stainless Steel Welds. *Metall Trans* 12A (1981) 213-223.
24. JA Brooks, AJ West and AW Thompson. Effect of Weld Composition and Microstructure on Hydrogen Assisted Fracture of Austenitic Stainless Steels. *Metall Trans* 14A (1983) 75-84.
25. RA Vandervoort. Tensile and Fracture Properties of Austenitic Stainless Steel 21-6-9 in High-Pressure Hydrogen Gas. *Metals Engineering Quarterly* 12 (1972) 10-16.
26. ASTM DS-56H, *Metals and Alloys in the UNIFIED NUMBERING SYSTEM* (SAE HS-1086 OCT01). American Society for Testing and Materials (Society of Automotive Engineers) (2001).
27. L Ma, G Liang, J Tan, L Rong and Y Li. Effect of Hydrogen on Cryogenic Mechanical Properties of Cr-Ni-Mn-N Austenitic Steels. *J Mater Sci Technol* 15 (1999) 67-70.

28. RE Stoltz and AJ West. Hydrogen Assisted Fracture in FCC Metals and Alloys. in: IM Bernstein and AW Thompson, editors. Proceedings of the International Conference on Effect of Hydrogen on Behavior of Materials: Hydrogen Effects in Metals, 1980, Moran WY. The Metallurgical Society of AIME (1980) p. 541-553.
29. RE Stoltz, NR Moody and MW Perra. Microfracture Model for Hydrogen Embrittlement of Austenitic Steels. Metall Trans 14A (1983) 1528-1531.

Table 1.1.1. Specification limits for 21-6-9 stainless steels and composition of several heats used to study hydrogen effects.

heat	Fe	Cr	Ni	Mn	Si	C	N	other	Ref.
UNS S21900	Bal	19.00 21.50	5.50 7.50	8.00 10.00	1.00 max	0.08 max	0.15 0.40	0.030 max S; 0.060 max P	[26]
UNS S21904	Bal	19.00 21.50	5.50 7.50	8.00 10.00	1.00 max	0.04 max	0.15 0.40	0.030 max S; 0.060 max P	[26]
UNS S21980	Bal	19.0 21.5	5.50 7.50	8.00 10.00	1.00 max	0.05 max	0.10 0.30	0.03 max S; 0.03 max P; 0.75 max Cu; 0.75 max Mo	[26]
V72	Bal	21.0	7.1	8.8	0.4	0.03	0.3	0.003 $\square$ ; 0.01 $\square$	[25]
O76a	Bal	19.90	7.53	8.70	0.17	0.033	0.12		[1]
O76b	Bal	19.70	7.60	8.63	0.19	0.040	0.24		
O76c	Bal	19.60	6.70	8.90	0.16	0.030	0.31		
O76d	Bal	20.10	7.12	8.55	0.19	0.035	0.43		
O76e	Bal	19.90	7.53	8.70	0.17	0.035	0.47		
H80	Bal	20.2	6.2	9.0	0.5	0.03	0.25	0.015 $\square$ ; 0.02 $\square$	[17]
P81	Bal	19.92	6.69	9.17	0.37	0.032	0.219		[19]
W82a	Bal	20.1	6.20	9.14	0.41	0.040	0.30	<0.01 $\square$ ; <0.02 $\square$	
W82b	Bal	19.7	7.29	8.63	0.23	0.023	0.28		
W82c	Bal	19.6	7.08	9.07	0.48	0.026	0.30		
W82d	Bal	19.5	7.36	8.73	0.25	0.018	0.28		
W82e	Bal	19.8	7.10	9.21	0.15	0.014	0.24		
B83aw	Bal	20.8	8.8	8.1	0.61	0.03	0.17	0.010 $\square$ ; 0.019 $\square$	[24]
B83bw	Bal	20.7	7.8	9.3	0.60	0.03	0.27	0.006 $\square$ ; 0.017 $\square$	[24]
C83	Bal	20.32	6.71	9.01	0.24	0.015	0.35	0.016 S; 0.018 $\square$	[7]
A87	Bal	20.9	7.1	8.8	0.44	0.035	0.37	0.005 $\square$ ; 0.010 $\square$	[20]
M91a	Bal	19.2	7.22	9.23	0.41	0.032	0.28	0.003 $\square$ ; 0.014 P	
M91b	Bal	19.4	6.40	8.50	0.33	0.040	0.28	<0.001 $\square$ ; 0.021 P	
M91c	Bal	20.1	6.50	9.10	0.59	0.037	0.29	<0.001 $\square$ ; 0.019 P	

w = composition of the weld fusion zone

Table 2.1. Average permeability and solubility relationships determined for several austenitic stainless steels, except Ref. [11] which is determined from hydrogen concentration measurements using hot extraction from 21-6-9 stainless steel thermally precharged from hydrogen gas.

Material	Temperature Range (K)	Pressure Range (MPa)	$P = P_o \exp(-E_p / RT)$		$S = S_o \exp(-E_s / RT)$		Ref.
			$P_o$ [ $\frac{\text{mol H}_2}{\text{m} \cdot \text{s} \cdot \sqrt{\text{MPa}}}$ ]	$E_p$ [ $\frac{\text{kJ}}{\text{mol}}$ ]	$S_o$ [ $\frac{\text{mol H}_2}{\text{m}^3 \cdot \sqrt{\text{MPa}}}$ ]	$E_s$ [ $\frac{\text{kJ}}{\text{mol}}$ ]	
Average of several austenitic alloys †	423-700	0.1-0.3	$1.2 \times 10^{-4}$	59.8	179	5.9	[14]
Based on >20 studies on 12 austenitic alloys	---	---	$3.27 \times 10^{-4}$	65.7	---	---	[12]
From hot extraction measurements on 21-6-9	---	---	---	---	346	8	[11]
Average of four austenitic alloys	373-623	$1 \times 10^{-4}$ - 0.03	$5.35 \times 10^{-5}$	56.1	266	6.86	[16]
Average of six austenitic alloys	473-703	0.1	$2.81 \times 10^{-4}$	62.27	488	8.65	[13]

† Data from Ref. [14] is determined for deuterium: permeability has been corrected here to give permeability of hydrogen (by multiplying by the square root of the mass ratio:  $\sqrt{2}$ ); solubility is assumed to be independent of isotope.

Table 2.2. Hydrogen solubility of 21-6-9 stainless steels measured from hot extraction after thermal precharging in hydrogen gas.

Material	Surface condition	Thermal precharging	Hydrogen concentration <sup>†</sup>		Ref.
			wppm	appm	
21-6-9, heat H80	---	69MPa H <sub>2</sub> 573K	109	6000	[17]
21-6-9 annealed	600 grit finish	69MPa H <sub>2</sub> 470K	118	6500	[15]
	Electropolished		126	6900	
21-6-9 HERF	600 grit finish		126	6900	
	Electropolished		127	7000	
21-6-9 CW	600 grit finish		119	6500	
	Electropolished		126	6900	
21-6-9 annealed	---	10MPa H <sub>2</sub> 573K	65	3600	[27]

HERF = high energy rate forging, CW = cold-work

<sup>†</sup> 1 wppm  $\approx$  55 appm

Table 3.1.1.1. Smooth tensile properties of 21-6-9 stainless steel at room temperature; measured in external hydrogen gas, or measured in air with internal hydrogen (thermal precharging in hydrogen gas), or measured in external hydrogen gas with internal hydrogen.

Material	Thermal precharging	Test environment	Strain rate (s <sup>-1</sup> )	S <sub>y</sub> (MPa)	S <sub>u</sub> (MPa)	El <sub>u</sub> (%)	El <sub>t</sub> (%)	RA (%)	Ref.
21-6-9, heat W82a HERF	None (1)	Air 172MPa H <sub>2</sub>	0.54 x 10 <sup>-3</sup>	889	993	20	46	68	[6]
				917	993	8	11	14	
21-6-9, heat W82b HERF	None None (1)	Air 172MPa H <sub>2</sub> 172MPa H <sub>2</sub>		654	882	38	52	74	
				703	924	30	43	67	
				731	917	30	40	48	
21-6-9, heat W82c HERF	None (1)	Air 172MPa H <sub>2</sub>		848	965	26	37	75	
				924	1062	21	31	64	
21-6-9, heat W82c HERF	None (1)	Air 172MPa H <sub>2</sub>		938	1000	12	30	62	
				951	993	16	28	53	
21-6-9, heat W82e HERF	None (1)	Air 172MPa H <sub>2</sub>		862	958	17	35	73	
				924	979	14	22	40	
21-6-9	None	Air		---	400†	670‡	---	58	
	None	69MPa He	---	350†	700‡	---	59	77	
	None	69MPa H <sub>2</sub>	---	360†	700‡	---	61	76	
21-6-9 CW 30%	None	Air	---	1240†	1290‡	---	26	53	[7]
	None	69MPa He	---	1010†	1050‡	---	26	63	
	None	69MPa H <sub>2</sub>	---	980†	1100‡	---	26	64	
	30MPa H <sub>2</sub>	Air	---	1075†	1150‡	---	32	35	
	30MPa H <sub>2</sub>	69MPa H <sub>2</sub>	---	1060†	1130‡	---	36	36	
21-6-9 HERF	None	Air	---	610†	790‡	---	34	74	[7]
	None	69MPa He	---	570†	780‡	---	34	75	
	None	69MPa H <sub>2</sub>	---	570†	790‡	---	30	73	
	30MPa H <sub>2</sub>	Air	---	660†	820‡	---	31	59	
	30MPa H <sub>2</sub>	69MPa H <sub>2</sub>	---	630†	830‡	---	31	54	

HERF = high energy rate forging, CW = cold work

† true stress at 5% strain

‡ true stress at maximum load

(1) 69MPa hydrogen gas, 473K, 240mm (gauge diameter 15mm); hydrogen concentration predicted to vary surface to center

Table 3.1.1.2. Smooth tensile properties of 21-6-9 stainless steel at room temperature; measured in air with internal hydrogen (thermal precharging in hydrogen gas).

Material	Thermal precharging	Test environment	Strain rate † (s <sup>-1</sup> )	S <sub>y</sub> (MPa)	S <sub>u</sub> (MPa)	EI <sub>u</sub> (%)	EI <sub>t</sub> (%)	RA (%)	Ref.
21-6-9	None	Air	---	434	689	---	56	56	[4]
	(1)	Air		441	724	---	30	28	
21-6-9 HERF	None	Air	---	607	793	---	32	74	[4]
	(2)	Air		655	820	---	31	59	
21-6-9, heat M91c annealed	None (3)	Air	8.5 x 10 <sup>-3</sup> mm/s†	500	811	---	80	75	[8]
		Air		555	839	---	83	60	
21-6-9, heat M91a HERF	None (3)	Air		712	932	---	40	71	
		Air		776	974	---	34	43	
21-6-9, heat M91a/b HERF	None (3)	Air		819	969	---	26	56	
		Air		1005	1093	---	28	33	
21-6-9, heat M91b HERF	None (3)	Air		825	1029	---	33	64	
		Air		836	948	---	---	---	
21-6-9, heat M91c HERF	None (3)	Air		918	1032	---	46	63	
		Air		965	1073	---	46	39	

† when strain rate is not known, displacement rates are quoted if reported

HERF = high energy rate forging

(1) 69 MPa hydrogen gas, 473K, 340h; hydrogen concentration of 8600ppm (47000ppm)

(2) 28 MPa hydrogen gas, temperature not specified, time specified as "prolonged"

(3) 69MPa hydrogen gas, 623K, 1000h (gauge diameter 4.8mm); calculated uniform hydrogen concentration of 1700ppm (9500ppm)

Table 3.1.1.3. Smooth tensile properties of a single heat of 21-6-9 stainless steel in different microstructural conditions at room temperature; measured in external hydrogen gas, or measured in external hydrogen gas with internal hydrogen (thermal precharging in hydrogen gas).

Material	Thermal precharging	Test environment	Strain rate (s <sup>-1</sup> )	S <sub>y</sub> (MPa)	S <sub>u</sub> (MPa)	El <sub>u</sub> (%)	El <sub>t</sub> (%)	RA (%)	Ref.
21-6-9, heat W82d annealed	None (1)	Air	0.54 x 10 <sup>-3</sup>	414	765	45	51	63	[6]
		172MPa H <sub>2</sub>		496	827	40	49	59	
21-6-9, heat W82d bar stock	None None (1)	Air		758	951	21	38	54	
		120MPa H <sub>2</sub>		765	931	19	29	51	
		172MPa H <sub>2</sub>		800	938	14	18	42	
21-6-9, heat W82d HERF	None None (1)	172MPa H <sub>2</sub>		834	965	10	11	22	
		Air		800	896	15	28	68	
		172MPa H <sub>2</sub>		827	903	12	34	66	
21-6-9, heat W82d CW plate	None (1)	172MPa H <sub>2</sub>		862	931	8	11	26	
		Air		834	917	12	23	69	
		172MPa H <sub>2</sub>		869	931	17	27	65	

HERF = high energy rate forging, CW = cold work

(1) 69MPa hydrogen gas, 473K, 240h (gauge diameter 3.2mm); hydrogen concentration predicted to vary surface to center

Table 3.1.1.4. Smooth tensile properties of 21-6-9 stainless steel at room temperature with varying nitrogen content (given in wt%); measured in external hydrogen gas with internal hydrogen (thermal precharging in hydrogen gas).

Material	Thermal precharging	Test environment	Strain rate (s <sup>-1</sup> )	S <sub>y</sub> (MPa)	S <sub>u</sub> (MPa)	El <sub>u</sub> (%)	El <sub>t</sub> (%)	RA (%)	Ref.
21-6-9, heat O76a (0.12N) annealed plate	None (1)	Air 69 MPa H <sub>2</sub>	3 x 10 <sup>-3</sup>	296	683	---	65	74	[1]
				296	683	---	58	59	
21-6-9, heat O76b (0.24N) annealed plate	None (1)	Air 69 MPa H <sub>2</sub>		386	745	---	58	72	
				401	732	---	62	57	
21-6-9, heat O76c (0.31N) annealed plate	None (1)	Air 43 MPa H <sub>2</sub>		434	745	---	56	56	
				441	724	---	30	28	
21-6-9, heat O76d (0.43N) annealed plate	None (1)	Air 69 MPa H <sub>2</sub>		490	780	---	55	67	
				503	785	---	21	29	
21-6-9, heat O76e (0.47N) annealed plate	None (1)	Air 69 MPa H <sub>2</sub>		510	790	---	56	67	
				509	796	---	18	28	

(1) 24.1 MPa hydrogen gas, 473 K, 240 min (gauge diameter 3.5 mm); surface concentration calculated to be 55 wppm (3000 appm)

Table 3.1.1.5. Smooth tensile properties of 21-6-9 stainless steel as a function of test temperature, measured in air with internal hydrogen (thermal precharging in hydrogen gas).

Material	Thermal precharging	Test environment	Strain rate (s <sup>-1</sup> )	S <sub>y</sub> (MPa)	S <sub>u</sub> (MPa)	EI <sub>u</sub> (%)	EI <sub>t</sub> (%)	RA (%)	Ref.
21-6-9, heat C83 bar stock	None (1)	Air 380 K	---	680† 690†	940‡ 1020‡	30 36	39 46	81 64	[7]
	None (1)	Air 298K		770† 800†	1170‡ 1270‡	41 46	51 56	80 60	
	None (1)	Air 250K		860† ---	1360‡ 1380‡	46 41	57 46	78 36	
	None (1)	Air 200K		970† 1060†	1550‡ 1650‡	48 44	58 48	79 48	
	None (1)	Liquid N <sub>2</sub> 77K		1580† 1600†	2140‡ 2060‡	45 36	49 36	47 32	
21-6-9 HERF	None (2)	Air 380 K	---	780† 690†	970‡ 930‡	21 26	31 33	69 49	[7]
	None (2)	Air 298K		780† 890†	1140‡ 1220‡	32 30	44 42	71 62	
	None (2)	Air 220K		900† 960†	1320‡ 1420‡	33 37	45 47	73 55	
	None (2)	Air 200K		1020† 990†	1610‡ 1740‡	42 53	54 60	72 48	
21-6-9 HERF	None (3)	Air 380 K	---	540† 570†	1040‡ 1070‡	47 50	59 68	84 72	[7]
	None (3)	Air 273K		640† 690†	1300‡ 1430‡	57 67	69 78	84 65	
	None (3)	Air 200K		930† 1050†	1700‡ 1830‡	51 49	59 54	72 59	
	None (3)	Liquid N <sub>2</sub> 78K		1450† 1400†	2840‡ 2600‡	46 46	56 46	56 41	

† true stress at 5% strain

‡ true stress at maximum load

(1) 69MPa deuterium gas, 620K, 500H

(2) 69MPa hydrogen gas, 620K, 500H

(3) 69MPa hydrogen gas, 470K, 35000H

Table 3.2.1.1. Fracture toughness of 21-6-9 stainless steel at room temperature; measured in external hydrogen gas, or measured in external hydrogen gas after exposure to hydrogen gas.

Material	Test method	Thermal precharging	Test environment	$S_y$ † (MPa)	$K_{Ic}$ ‡ (MPa)	Ref.
21-6-9 HERF, Longitudinal	C-specimen	None	690 MPa He	---	79	[7]
		None	690 MPa H <sub>2</sub>	---	81	
		0.6 MPa H <sub>2</sub>	690 MPa H <sub>2</sub>	---	76	
21-6-9 HERF, Transverse	C-specimen	None	690 MPa He	---	74	[7]
		None	690 MPa H <sub>2</sub>	---	68	
		0.6 MPa H <sub>2</sub>	690 MPa H <sub>2</sub>	---	62	

HERF = high energy rate forging

† yield strength of smooth tensile specimen

‡ not clear if plane strain requirements are met in these studies

Table 3.2.2.1. Threshold stress intensity factor of 21-6-9 stainless steel; measured in external hydrogen gas.

Material	$S_y$ † (MPa)	RA † (%)	Threshold Stress Intensity Factor (MPa m <sup>1/2</sup> )		Ref.
			100 MPa H <sub>2</sub>	200 MPa H <sub>2</sub>	
21-6-9, heat P81 HERF (11130K, WQ)	827	36	103	99*	[19] ‡

HERF = high-energy rate forging, WQ = water quench

† yield strength and reduction in area of smooth tensile specimen, not exposed to hydrogen

\* did not satisfy plane strain requirements for analysis of linear elastic fracture mechanics

‡ data also reported in Ref. [28, 29]

Table 3.5.1. Impact fracture data for 21-6-9 stainless steel with internal hydrogen (thermal precharging in hydrogen gas).

Material	Specimen	Thermal precharging	Test environment	$S_y$ † (MPa)	Impact Energy (J)	Ref.
21-6-9	(a)	None	Liquid N <sub>2</sub>	---	37	[7]
		(1)	77 K	---	35	
HERF	(a)	None	Air 2980K	---	110	
		(1)		---	91	

HERF = high-energy rate forging

† yield strength of smooth tensile specimen, not exposed to hydrogen

(a) modified Naval Research Laboratory dynamic tear specimen [7]

(1) 29.6 MPa hydrogen gas, 4700K, 13000K

Table 4.2.1. Smooth tensile properties of sensitized 21-6-9 stainless steel at room temperature, measured in external hydrogen gas with internal hydrogen (thermal precharging in hydrogen gas).

Material	Thermal precharging	Test environment	Strain rate (s <sup>-1</sup> )	S <sub>y</sub> (MPa)	S <sub>u</sub> (MPa)	El <sub>u</sub> (%)	El <sub>t</sub> (%)	RA (%)	Ref.
21-6-9, heat W82a HERF	None	Air	0.54 x 10 <sup>-3</sup>	834	965	18	39	73	[6]
	(1)	70 MPa H <sub>2</sub>		882	986	17	32	57	
	(1)	120 MPa H <sub>2</sub>		882	1007	15	20	35	
	(1)	172 MPa H <sub>2</sub>		882	993	11	15	28	
21-6-9, heat W82a HERF + S	None	Air		813	951	10	29	68	
	None	172 MPa H <sub>2</sub>		800	944	13	28	73	
	(1)	70 MPa H <sub>2</sub>		869	986	9	25	50	
	(1)	120 MPa H <sub>2</sub>		882	1007	6	10	23	
	(1)	172 MPa H <sub>2</sub>		869	972	5	10	21	

HERF = high energy rate forging, S = sensitized

(1) 69 MPa hydrogen gas, 473 K, 240 h (gauge diameter 3.5 mm); hydrogen concentration predicted to vary surface to center

Table 4.3.1. Smooth tensile properties of 21-6-9 stainless steel composite GTA weld specimens at room temperature; measured in external hydrogen gas, or measured in air with internal hydrogen (thermal precharging in hydrogen gas), or measured in external hydrogen gas with internal hydrogen.

Material	Thermal precharging	Test environment	Strain rate (s <sup>-1</sup> )	S <sub>y</sub> (MPa)	S <sub>u</sub> (MPa)	El <sub>u</sub> (%)	El <sub>t</sub> (%)	RA (%)	Ref.
21-6-9 HERF/ 308L filler wire GTA welds, heat B83aw ‡	None	Air	0.33 x 10 <sup>-3</sup>	539	746	9.7	14	54	[24]
	None	69MPa H <sub>2</sub>		534	738	10	14	57	
	None	172MPa H <sub>2</sub>		573	786	11	15	61	
	(1)	Air		553	757	8.8	12	49	
	(1)	69MPa H <sub>2</sub>		---	756	---	---	43	
	(2)	Air		579	776	10	12	44	
21-6-9 HERF/ 21-6-9 filler wire GTA welds, heat B83bw ‡	None	Air	0.33 x 10 <sup>-3</sup>	530	773	12	19	60	[24]
	None	69MPa H <sub>2</sub>		498	754	14	22	75	
	None	172MPa H <sub>2</sub>		543	795	12	20	69	
	(1)	Air		514	769	13	18	56	
	(1)	69MPa H <sub>2</sub>		612	827	---	---	50	
	(2)	Air		543	789	12	16	50	
	(2)	172MPa H <sub>2</sub>	589	842	14	17	49		

HERF = high energy rate forging, GTA = gas tungsten arc

‡ The base material for these studies was HERF, back extrusions of 21-6-9, machined to cylindrical shape (10mm diameter, 1.5mm wall thickness) with circumferential double J grooves; eight to ten GTA weld passes were required to fill groove. The filler wire material was either 308L or 21-6-9. Tensile bars contain base material and heat affected zone with the fusion zone centered in the gauge length.

(1) 24MPa hydrogen gas, 473K, 240h: calculated concentration gradient of 45 to 4 wppm surface to center (2500 to 200ppm)

(2) 69MPa hydrogen gas, 473K, 240h: calculated concentration gradient of 72 to 7 wppm surface to center (4000 to 400ppm)

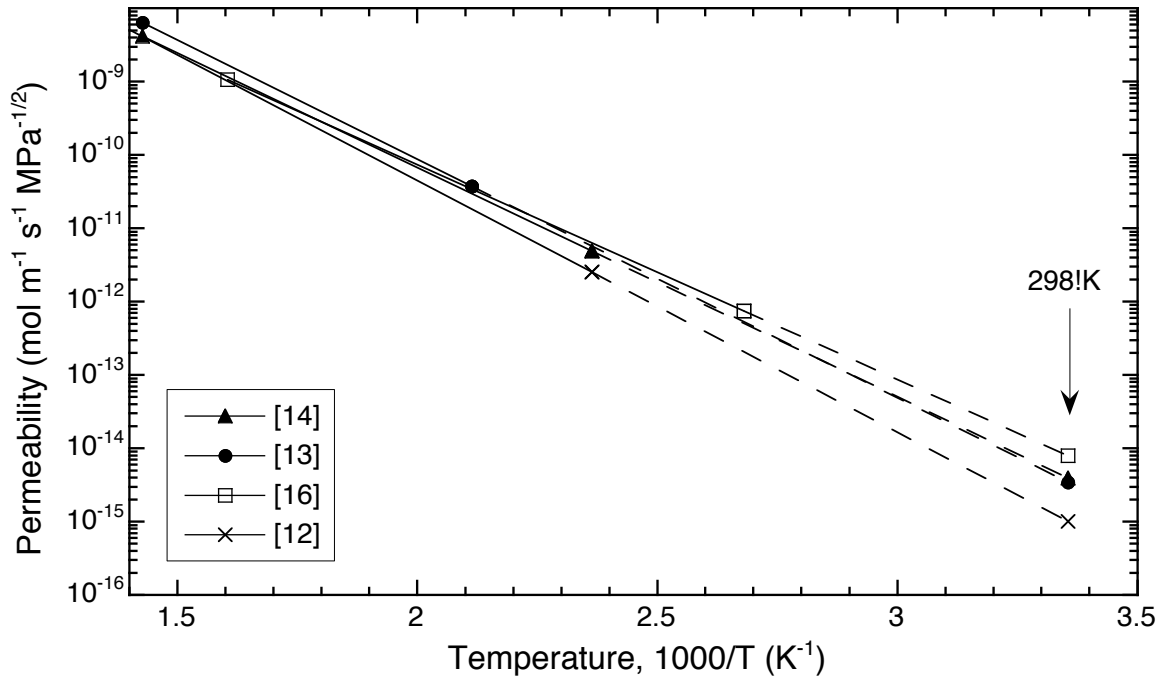


Figure 2.1. Permeability relationships (from Table 2.1) for austenitic stainless steels extrapolated (dashed lines) to  $298 \text{ K}$ . Permeability from Ref. [14] was determined for deuterium and has been corrected to give permeability of hydrogen by multiplying by the square root of the mass ratio:  $\sqrt{2}$ .

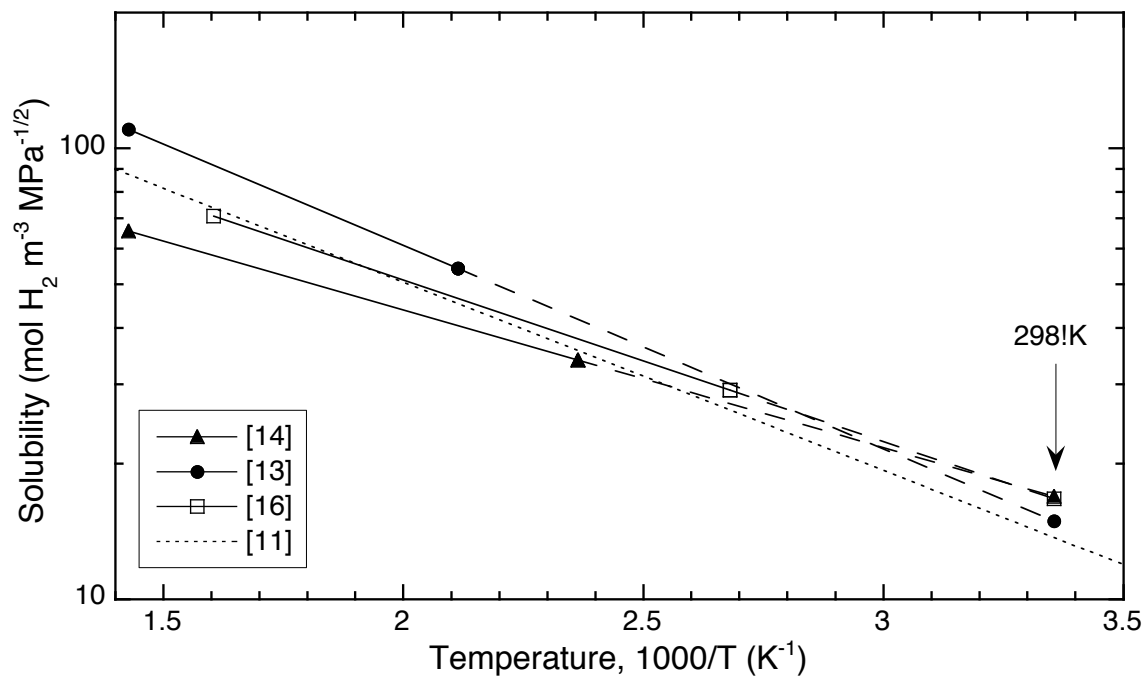


Figure 2.2. Solubility relationships (from Table 2.1) extrapolated (dashed lines) to  $298 \text{ K}$  and determined from permeability and diffusivity data for austenitic stainless steels. Data from Ref. [14] are for deuterium.

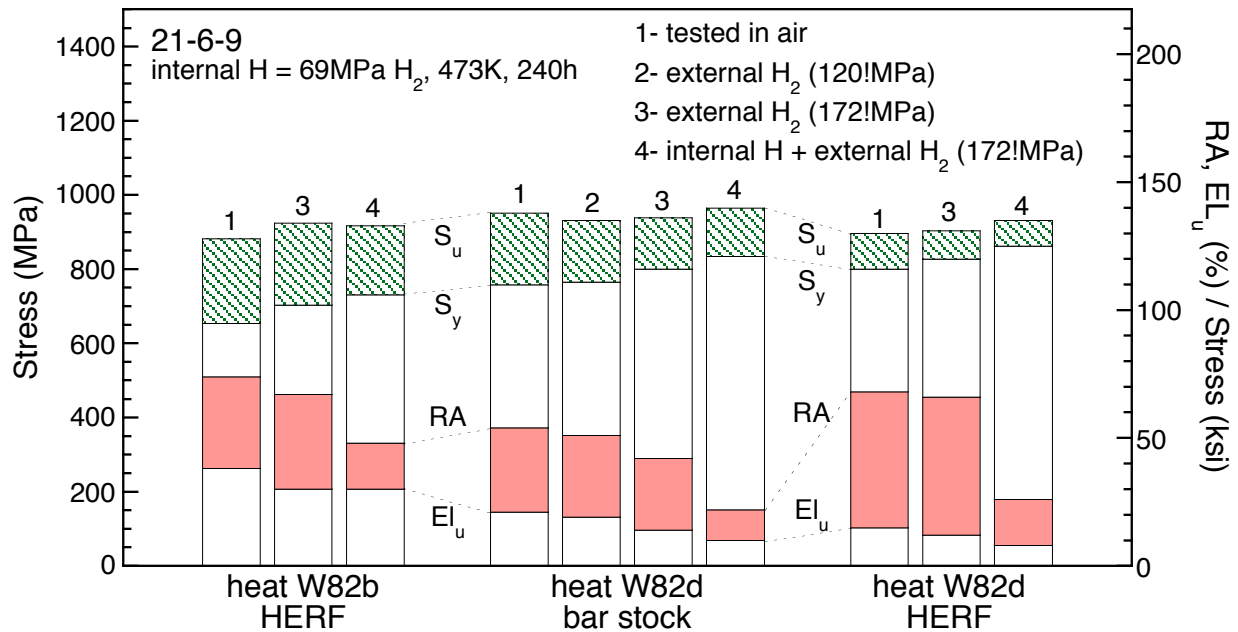


Figure 3.1.1.1. Smooth tensile properties of 21-6-9 stainless steel: (1) tested in air; (2, 3) tested in external hydrogen gas; and (4) tested in external hydrogen gas with internal hydrogen. [6]

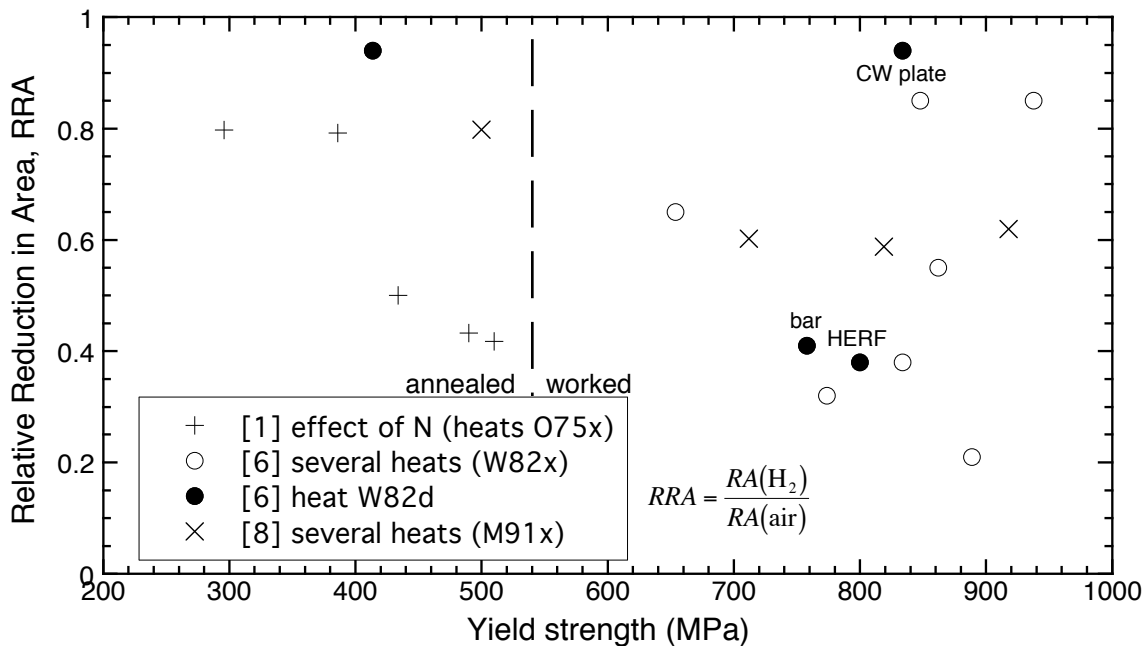


Figure 3.1.1.2. Relative reduction in area (smooth tensile) of 21-6-9 stainless steels as a function of yield strength. Ref. [1]: tested in external hydrogen gas (69MPa) with internal hydrogen (24MPa hydrogen gas at 473K: non-uniform). Ref. [6]: tested in external hydrogen gas (172MPa) with internal hydrogen (69MPa hydrogen gas at 473K: non-uniform). Ref. [8]: tested in air with internal hydrogen (69MPa hydrogen gas at 623K: uniform).

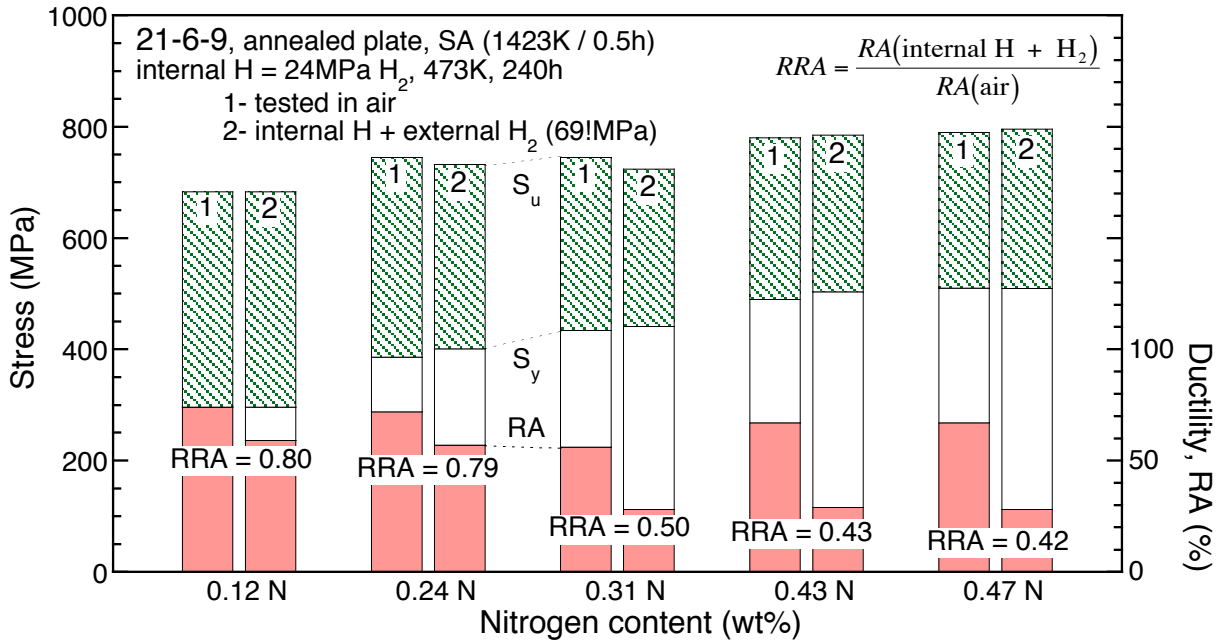


Figure 3.1.1.3. Smooth tensile properties of solution-annealed (SA) 21-6-9 stainless steel with varying nitrogen content, heats 075a-e; measured in external hydrogen gas with internal hydrogen (thermal precharging in hydrogen gas). [1]

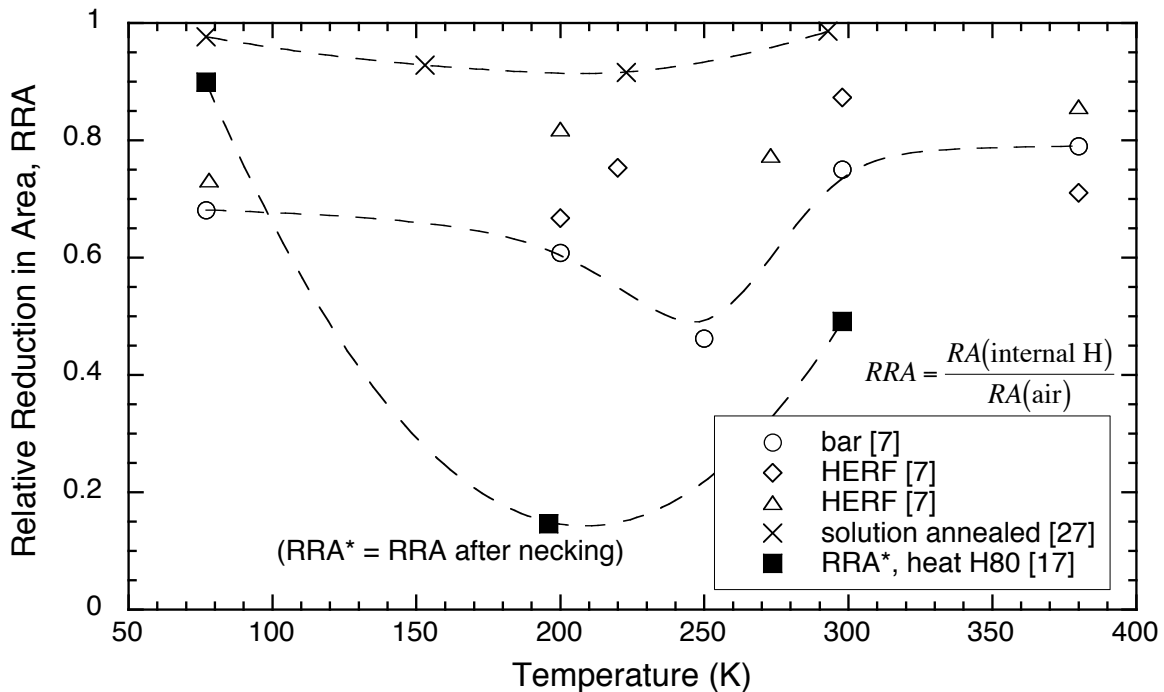


Figure 3.1.1.4. Relative reduction in area (smooth tensile) of several heats of 21-6-9 stainless steel as a function of test temperature; with internal hydrogen. Data from Ref. [7] also given in Table 3.1.1.2. Precharging conditions: Ref. [7], 21-6-9 bar, 69 MPa D<sub>2</sub> at 620K; 21-6-9 HERF, 69 MPa H<sub>2</sub> at 620K; 21-6-9 HERF, 69 MPa H<sub>2</sub> at 470K; Ref. [27], 10MPa H<sub>2</sub> at 573K (uniform); Ref. [17], 69MPa H<sub>2</sub> at 573K (uniform).

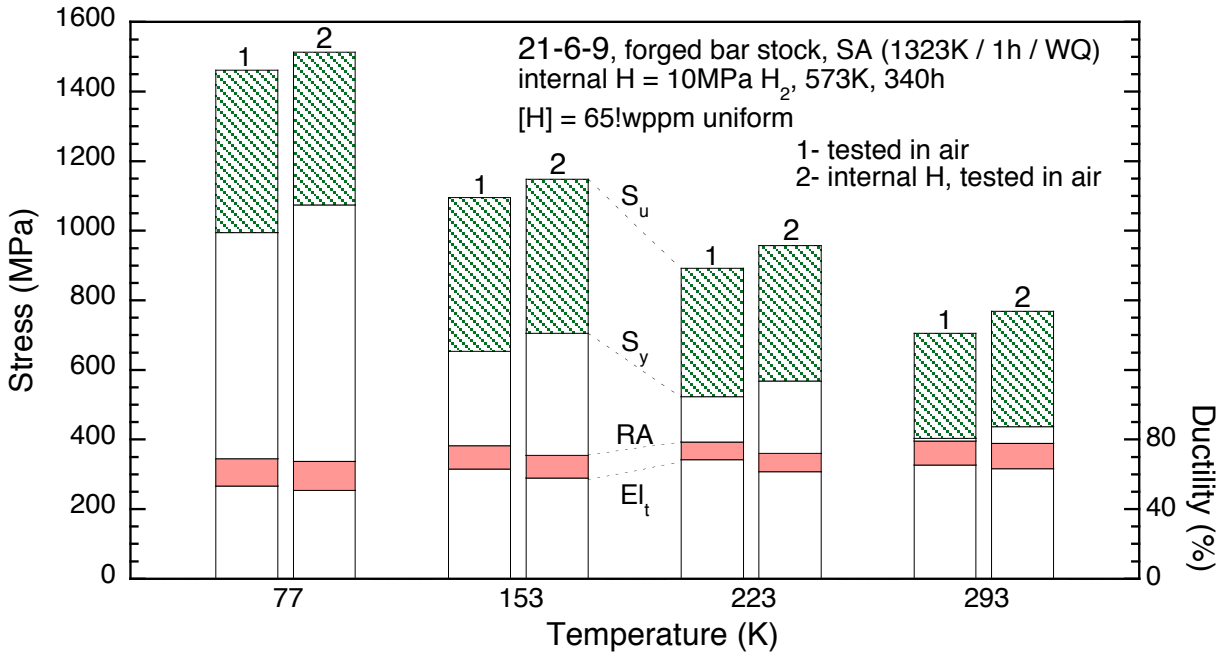


Figure 3.1.1.5. Smooth tensile properties of solution-annealed (SA) 21-6-9 stainless steel as a function of test temperature; measured in air with internal hydrogen (thermal precharging in hydrogen gas). [27]

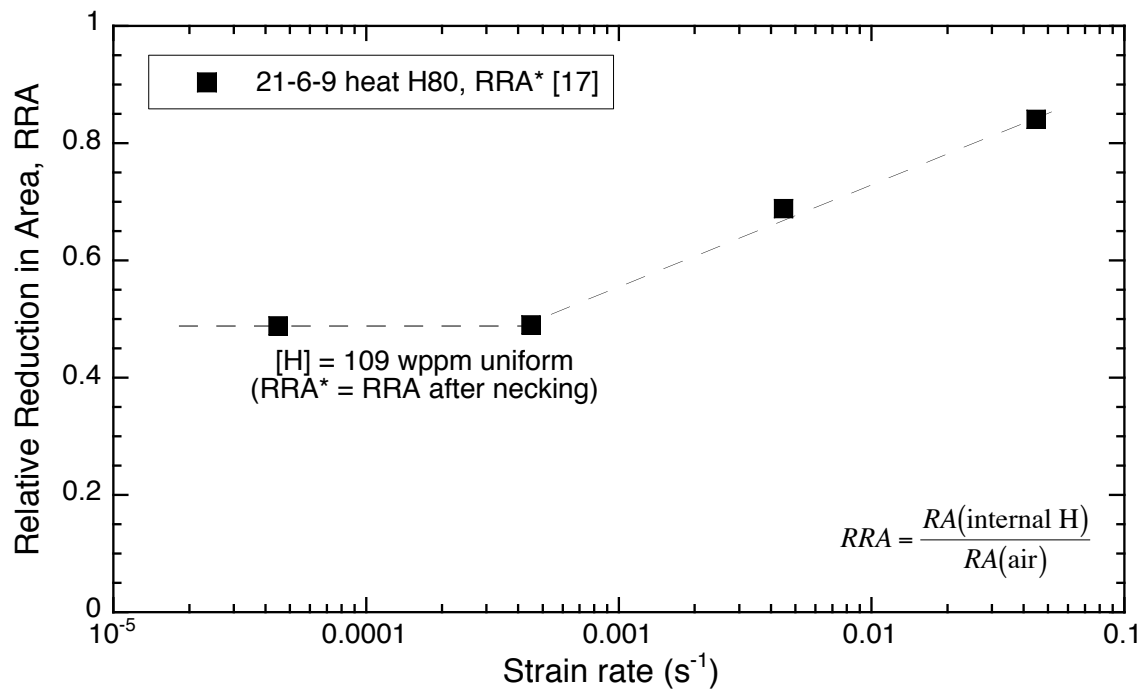


Figure 3.1.1.6. Relative reduction in area (smooth tensile) of 21-6-9 stainless steel (heat H80) as a function of strain rate; measured in air with internal hydrogen (thermal precharging in hydrogen gas). Precharging conditions: Ref. [17], 69MPa H<sub>2</sub> at 573K (uniform).

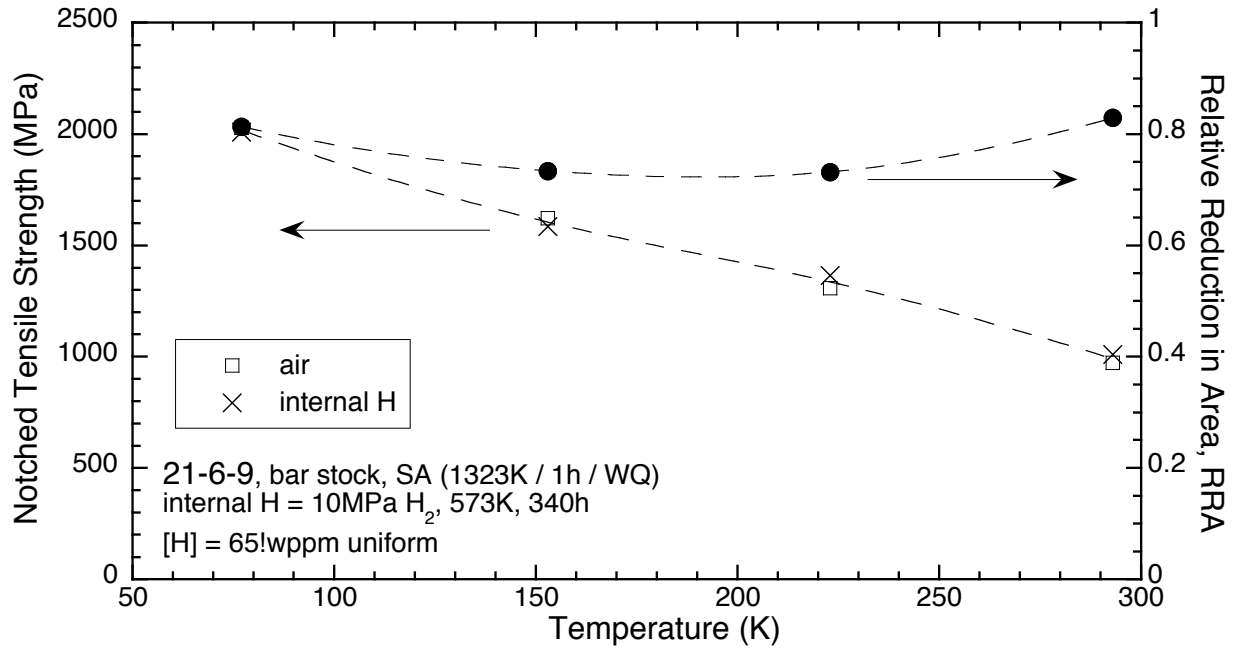


Figure 3.1.2.1. Notched tensile properties of 21-6-9 SA bar stock. Notched specimen: stress concentration factor ( $K_t$ ) = 4.55; notch geometry = 60° included angle; minimum diameter = 4mm; maximum diameter = 5mm; notch root radius = 0.1mm; crosshead rate = 4.2x10<sup>-2</sup> mm/s. SA = solution annealed, WQ = water quench. [27]

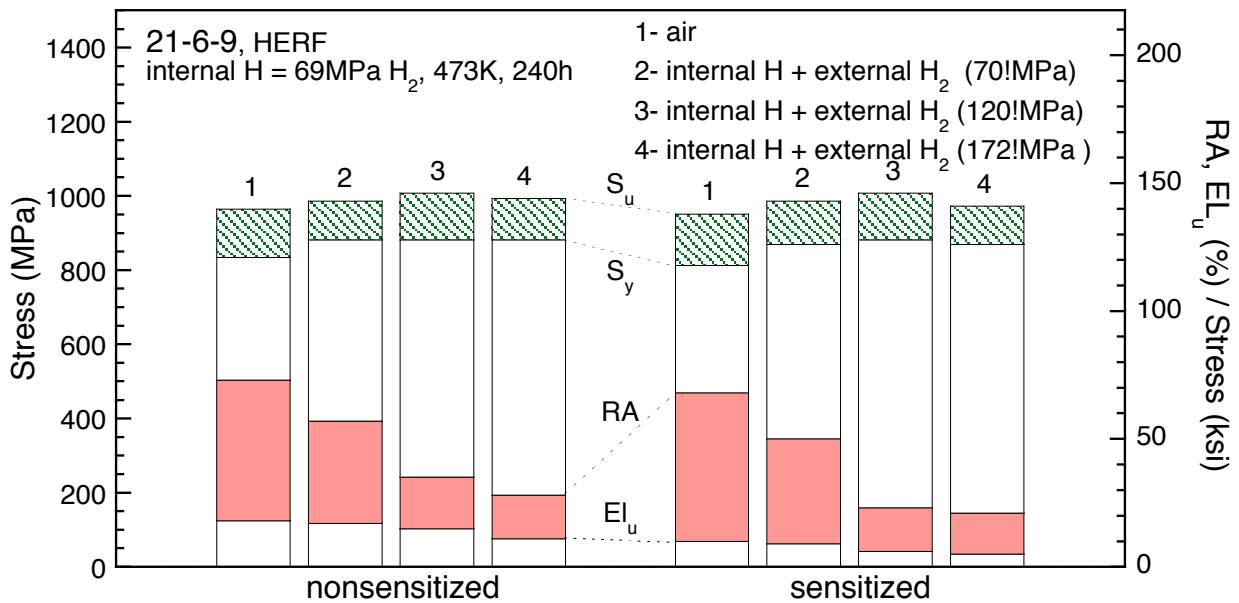


Figure 4.2.1. Smooth tensile properties of 21-6-9 stainless steel that has been sensitized; sensitization conditions are not known; measured in hydrogen gas with internal hydrogen (thermal precharging in hydrogen gas). [6]